Physica A 541 (2020) 123605

Contents lists available at ScienceDirect

Physica A

journal homepage: www.elsevier.com/locate/physa

Sparse Bayesian learning for network structure reconstruction based on evolutionary game data

Keke Huang *, Wenfeng Deng, Yichi Zhang *, Hongqiu Zhu

School of Automation, Central South University, Changsha 410083, China

ARTICLE INFO

Article history:
Received 1 September 2019
Received in revised form 28 October 2019
Available online 6 December 2019

Keywords:
Network structure reconstruction
Evolutionary game
Compressed sensing
Sparse Bayesian learning

ABSTRACT

Network structure reconstruction is a fundamental problem for understanding, predicting and controlling the behaviors of complex networked systems and has received growing attention due to the potentials in a wide range of fields. Recent years have witnessed dramatic advances in the field of network structure reconstruction, especially the famous compressed sensing-based methods. However, some neglected disadvantages still exist in the existing works, such as the high measurement correlation existing in the solution matrix, reconstruction behaviors subject to model-based constraints and pure point estimate of the reconstruction results without credibility, which inevitably drag down the reconstruction performance. To address these problems, we propose a new framework of sparse Bayesian learning for network structure reconstruction based on evolutionary game data from the perspective of Bayesian and statistics. Specifically, we formulate the problem of network structure reconstruction as a Bayesian compressed sensing problem. Then, a hierarchical prior model is invoked for conjugated Bayesian inference to obtain the posterior distribution of the reconstructed result, including the reconstructed mean and covariance. Finally, the parameters in the reconstructed results are updated by an iterative estimation procedure. Results from numerical experiments have demonstrated applicability and efficiency of the proposed method and presented superiority over other reconstruction methods.

1. Introduction

Complex networked systems widely exist in various fields of science and engineering [1–3] such as gene regulatory networks [4], epidemic spreading networks [5], social interaction networks [6], transportation networks [7] and etc. An accepted idea shared among different scientific communities is that to provide a comprehensive understanding of the complex networked system, it is imperative to explore it as a whole rather than separate it into components [2,8]. Besides, gaining full knowledge of underlying structures can provide valuable guidance to predict and control the behaviors of networked systems [9]. However, a big challenge is that for various reasons, the physical link connections or patterns of node-to-node interactions within networks such as neural network and protein network, are totally unknown or unobservable often, but only limited time series data are available in practice [6,10], bringing obstacles for overall analysis and exploration in a wide variety of fields. Thus, it is of both theoretical significance and practical value to uncover the underlying structures of complex networked systems [9].

* Corresponding authors.
E-mail addresses: huangkeke@csu.edu.cn (K. Huang), zndxzyc@csu.edu.cn (Y. Zhang).

https://doi.org/10.1016/j.physa.2019.123605
0378-4371/

As one of the central issues and fundamental inverse problem in complex networked system, data-based network structure reconstruction plays an utmost significant role in interdisciplinary fields and attracts continuous interest, whose goal is to uncover the underlying topological structure of networks based on measurement data [11–14]. In fact, network structure reconstruction with very few available data is an important and challenging task, especially in the rigorous environment of data measuring and sampling. Not only that, the strong coherence of sampling data and the influence of strong noise mixed in practical systems are grave threats, leading to deterioration in network structure reconstruction inevitably. So the reconstructed structure is of large deviation and lacks enough credibility, which makes it a knotty problem in practice. Recent years have witnessed dramatic advances in the field of network structure reconstruction, among of which are the famous compressed sensing-methods. For example, Shen et al. [5] developed a general theoretical framework of reconstructing the complex propagation networks and identifying hidden sources via compressed sensing theory. Wang et al. [6] proposed a compressed sensing-based framework for uncovering network topology network based on evolutionary-game data. Li et al. [9] proposed a new method to recover topological structure of complex networks by combining different orders of Taylor expansion and compressed sensing for a more common situation where the basis functions of network node dynamics are unknown. Huang et al. [15] introduced a novel improvement technique for network structure reconstruction in the framework of compressed sensing. Su et al. [16] presented a compressed sensing-based approach to infer the existence and locations of hidden nodes in complex networks.

Although current research on compressed sensing-based network structure reconstruction has received considerable attention, some neglected disadvantages still exist, which inevitably drag down the performance to some extent. Specifically, in most compressed sensing-based reconstruction process, high measurement correlation exists in the solution matrix in most kinds of dynamics and the reconstruction behaviors depend heavily on the model-based constraints, e.g. *restricted isometry property* (RIP) [17] and the mutual coherence [18], leading to non-optimal local solutions in the reconstruction process and undoubtedly weakening the reconstruction performance. In addition, due to the existence of noise in the sampling measurement data or other unexpected factors, such as stochastic forces on physical systems and noisy environments, pure point estimate of the reconstruction result is inevitably short of credibility, causing deviation and less confidence of real results.

Sparse Bayesian learning, as one important family of Bayesian algorithms, was first proposed by Tipping [19] in the context of *relevance vector machine* (RVM), which has received increasing attention in recent years due to its great performance in many applications [20–23]. Recently, there has emerged a boom of research in the field of sparse Bayesian learning. For example, Wipf and Rao [24] introduced sparse Bayesian learning to the signal processing problem for finding sparse representations of signals from overcomplete dictionaries. Zhang et al. [25] proposed a block sparse Bayesian learning framework to address the sparse signal recovery problem where temporal correlation exists in the solution matrix and achieved superior signal recovery performance. Fang et al. [26] developed a sparse Bayesian learning method in the scene of recovering block-sparse signals with unknown cluster patterns. To the best of our knowledge, few works have studied the scenario of network structure reconstruction from the perspective of Bayesian and statistics. In the scene of the inverse problem, a statistical model which takes the sparse signal, as well as the effect of noise into account at the same time can make the best of the noise statistics model as prior information to deal with the strong coherence and high noise level of the solution matrix. Besides, as this model does not require to solve the problem of obtaining a singular value or eigenvalue [27], what we need to solve is a root-finding problem, which can get free from the model-based constraints in the reconstruction behaviors and avoids deterioration in high noise level [28]. Therefore, the reconstruction results are more applicable and general.

In this paper, we develop a new framework of sparse Bayesian learning for network structure reconstruction based on evolutionary game data. More specifically, we first formulate the compressed sensing problem with sampling data generated in networked prisoner's dilemma. Then, with the assumption of Gaussian distribution for sampling noise, the compressed sensing problem of inverting for the underlying topological structure of network is transformed into a Bayesian linear-regression analysis with the constraint of natural sparsity of network. After that, a hierarchical prior model is invoked for conjugated Bayesian inference. Finally, an iterative estimation procedure will be implemented for updating unknown parameters, yielding reconstructed mean and covariance from the posterior distribution, wherein the mean represents the point estimate of the reconstructed underlying topological structure and the covariance reflects the credibility of estimation. Numerical Results in the experiments demonstrate the applicability and efficiency of the proposed method from aspects of data requirement, performance under different network scales and robustness against strong noise. Furthermore, comparisons with some state-of-the-art network structure reconstruction algorithms, e.g., Lasso [7], Basic Pursuit(BP) [29], Orthogonal Matching Pursuit(OMP) [30], Iterative Shrinkage-Thresholding Algorithm(ISTA) [31], highlight the advantages of the proposed method and present superiority over other network structure reconstruction methods with better reconstruction performance. The contributions of this paper includes: (a) Formulate the problem of network topology reconstruction based on evolutionary game data as a Bayesian compressed sensing problem in the framework of sparse Bayesian learning from the perspective of Bayesian and statistics; (b) Consider a more realistic scenario of network structure reconstruction, where not only the point estimate of reconstruction result is provided, but also the covariance is given as the inferring confidence.

The remainder of this paper is structured as follows. Section 2 introduces the mathematical model, including the knowledge of networked prisoner's dilemma, compressed sensing basis, and sparse Bayesian learning-based network

structure reconstruction. Section 3 presents the numerical results and discussions. Finally, the conclusions and future work are given in Section 4.

Notation

Throughout this paper, denote by A^T the transpose of matrix A where T represents the symbol of transposition, and by $vec(\cdot) : \mathbb{R}^{M\times N} \to \mathbb{R}^{MN}$ the function that vectorizes a matrix column-by-column. The diagonal entries of the diagonal matrix A is denoted by diag(A). The function $\|\chi\|_1$, as referred to as the ℓ_1 norm, returns the sum of the absolute value of each element in vector χ. Denote by $\mathbf{v}_i$ the ith column of matrix $\mathbf{V}$ while v_i the ith entry of $\mathbf{v}_i$. Besides, we use subscript $i = 1, \ldots, N$ to denote the ith entry of a vector with dimension of $\mathbb{R}^N$.

2. Mathematical model

2.1. Networked prisoner's dilemma

The emergence of cooperation is a ubiquitous phenomenon in the real world, ranging from biological systems to social systems [32,33]. Additionally, cooperation has played a key role in supporting the evolution of biological systems at all levels of organizations, fascinating researchers from kinds of disciplines [34]. So far, as a well-known powerful mathematical tool, evolutionary game theory has presented a competent framework for studying the evolution of cooperation in communities of self-regarding agents and it has been extended to many related practical applications [35–38]. Moreover, it has proved that cooperation can be conveniently formalized in the framework of evolutionary game theory [39–42], wherein a lot of games have been developed as metaphors, such as the prisoner's dilemma in particular. Therefore, due to its wide applicability in describing various systems, evolutionary game dynamics is the best choice of dynamics model in our problem, which will be used to generate time series for the following analysis.

As one of the most commonly employed games for investigating the widespread cooperative behaviors among unrelated individuals, the prisoner's dilemma has received considerable attention and motivated a flurry of researches [34,43,44]. Generally, in a networked prisoner's dilemma, both of two equivalent players in a mutual interaction have two pure strategies (S) to adopt, called cooperation (C) or defection (D). For convenience, the strategy to cooperate or to defect are denoted by $S(C) = (1, 0)^T$ and $S(D) = (0, 1)^T$ mathematically, where T represents the symbol of transposition. Each player will interact with its opponents and then gain payoff from the interaction, which is determined by the strategies of them and the payoff matrix, expressed by the following 2×2 matrix in agreement with four possibilities

$$P_{PD} = \begin{pmatrix} R & S \\ T & P \end{pmatrix} \tag{1}$$

where the reward R represents the case of mutual cooperation whereas the punishment P for mutual defection. Rest of the two possibilities occur if players follow different strategies, where the cooperator gets the "sucker's" payoff S while the defector receives the payoff T characterizing the temptation to defect, wherein the ranking of $T > R > P > S$ and $2R > T + S$ holds and $1 < T < 2$ keeps the essentials of the prisoner's dilemma [45]. Without loss of generality, the parameters of the payoff matrix are set to $R = 1$, $T = 1.2$, $S = -0.15$ and $P = 0.04$. It is worth noting that under the constraints of game parameters, choosing a set of game parameters which contains both positive and negative value can make time series data generated in the dynamics process more comprehensive and close to the practical data in real systems. In addition, the game parameter setting in the payoff matrix will only affect the time series data generated, but the conclusions can still be consistent with those in this paper as long as the constraints of game parameters are guaranteed.

In networked prisoner's dilemma, all nodes occupied by players will play games with their direct neighbors and gain payoffs at each round. Summing over contributions from neighboring nodes leads to the total payoffs of the focal node. Specifically, at round t, the total payoff of node i from the networked prisoner's dilemma can be expressed as

$$U_i(t) = \sum_{j\in\delta_i} S_i^T(t) \cdot P_{PD} \cdot S_j(t) \tag{2}$$

where δ_i represents the set of node i's neighbors meanwhile $S_i(t)$ and $S_j(t)$ denote the strategies of node i and j at round t respectively. Afterwards, aiming to maximize the payoffs at the next round, all of self-centered players will consider updating their strategies by referring to the payoffs of their own and their neighbors' in the previous round according to the strategy updating mechanism, such as the best-take-over rule, random-selection rule, Fermi rule, etc. Here, we choose the most frequently used Fermi rule in this paper. To be concrete, player i will follow one of its neighbor's strategy randomly, denoted by $S_j(t)$ without loss of generality, with probability depending on the payoff difference $U_i(t) - U_j(t)$ at the current round as

$$W_{S_i(t+1)\leftarrow S_j(t)} = \frac{1}{1 + \exp\left[(U_i(t) - U_j(t))/\kappa\right]} \tag{3}$$

where κ characterizes the measure of stochastic uncertainties permitting irrational choices occasionally. Extreme case is that the strategy of those who possess higher payoff is absolutely dominant in the strategy updating episode when $\kappa = 0$. However, if $\kappa{=}\infty$, there leads to a completely random decision-making process regardless of the payoff difference. Similar to the parameter settings in literature [11,46], κ is set to 0.1 in the following research for simplicity.

2.2. Compressed sensing basis

Over the past few years, a new framework called compressed sensing (CS) in the signal processing community has emerged for simultaneous sampling and compression. It is built upon the pioneering work by Candes et al. [47] and Donoho [48] and has attracted considerable research interests in the field of science and engineering [49]. The main principle of CS lies on the fact that for the reasonably sparse or approximately sparse signal which is considered having sparse property in an appropriate basis, that is, only a few large coefficients containing the salient information exist in the signal while the other coefficients are equal or close to zero, can be captured by a small amount of linear projections [50]. Therefore, it is possible to reconstruct the raw signal of interest with high quality from fewer observations than traditionally assumed, avoiding redundant power consumption and computation complexity [49].

The conventional CS theory demonstrates that suppose a compressible original signal $\mathbf{x} \in \mathbb{R}^N$ with sparsity property, one can only acquire M linear measurements rather than all of N entries ($M \ll N$) in $\mathbf{x}$ under suitable conditions by using a $M \times N$ matrix, which can be expressed by a matrix–vector multiplication form

$$\mathbf{y} = \mathbf{\Phi x} \tag{4}$$

where $\mathbf{y} \in \mathbb{R}^M$ represents the sampled vector and $\mathbf{\Phi} \in \mathbb{R}^{M \times N}$ is the so-called measurement matrix. In other words, in case the original signal is sparse or can be made sparse with transformation (i.e. compressibility), and the measurement matrix satisfies conditions such as *restricted isometry property* (RIP) [51], it can be precisely recovered with overwhelming probability by using an ideal recovery procedure called ℓ_1 optimization [47].

$$\begin{aligned} &\arg\min_{\mathbf{x}\in\mathbb{R}^N} \|\mathbf{x}\|_1 \\ &s.t. \mathbf{y} = \mathbf{\Phi x} \end{aligned} \tag{5}$$

where $\|\cdot\|_1$ denotes the sum of the absolute value of each element in $\mathbf{x}$. In practice, inspired by the natural sparsity of most network topology structure, some related works have been devoted to explore the effectiveness of CS in network structure reconstruction problems and achieved quite outstanding results [6,15].

More generally, a robust mathematical model which takes noise into account [52] is considered quite often for the sake of accuracy in a specific acquisition system, which can be expressed in the form as

$$\mathbf{y} = \mathbf{\Phi x} + \mathbf{v} \tag{6}$$

where $\mathbf{v}$ stands for an unknown noise vector in agreement with the dimension of sampling vector. Hence, a modified convex optimization called Lasso can be implemented to address this problem [7,15] with detailed form as

$$\arg\min_{\mathbf{x}\in\mathbb{R}^N} \|\mathbf{x}\|_1 + \lambda \|\mathbf{y} - \mathbf{\Phi x}\|_2^2 \tag{7}$$

where λ represents a regularization parameter to avoid large deviation from the optimal solution [53]. In particular, the sparsity of the solution is ensured by the former item $\|\mathbf{x}\|_1$ meanwhile the latter item $\|\mathbf{y} - \mathbf{\Phi x}\|_2^2$ makes the solution more robust against noise originating from time series or missing data of partial nodes [7,48].

The key to network structure reconstruction problem is to establish an adjacency matrix $\mathbf{A}$ called "golden standard" [15], which contains details of link connections between nodes where $a_{ij} = 1$ if node i and j are connected and $a_{ij} = 0$ otherwise. Eq. (2) shows the payoff of node i is determined by the payoff matrix and strategies of i and its neighbors'. Considering the condition of link connections among all nodes, the payoff representation of node i can be rewrite specifically as

$$U_i(t) = \sum_{j \in \Xi} x_{ij} \cdot S_i^T(t) \cdot P_{PD} \cdot S_j(t) \tag{8}$$

where Ξ denotes the set of nodes in the network and x_{ij} denotes the link connection between node i and j. Thus, the reconstruction formula for node i with M accessible time instances, i.e., $t_1, \ldots, t_M$, can be expressed by a similar form of $\mathbf{y}_i = \mathbf{\Phi}_i \mathbf{x}_i$

$$\begin{pmatrix} U_i(t_1) \\ U_i(t_2) \\ \cdots \\ U_i(t_M) \end{pmatrix} = \begin{pmatrix} \phi_{i,1}(t_1) & \phi_{i,2}(t_1) & \cdots & \phi_{i,N}(t_1) \\ \phi_{i,1}(t_2) & \phi_{i,2}(t_2) & \cdots & \phi_{i,N}(t_2) \\ \cdots & \cdots & \cdots & \cdots \\ \phi_{i,1}(t_M) & \phi_{i,2}(t_M) & \cdots & \phi_{i,N}(t_M) \end{pmatrix} \begin{pmatrix} x_{i,1} \\ x_{i,2} \\ \cdots \\ x_{i,N} \end{pmatrix} \tag{9}$$

where the sampling payoff vector

$$\mathbf{y}_i = \begin{pmatrix} U_i(t_1) & U_i(t_2) & \cdots & U_i(t_M) \end{pmatrix}^T \tag{10}$$

the sampling strategy matrix

$$\mathbf{\Phi}_i = \begin{pmatrix} \phi_{i,1}(t_1) & \phi_{i,2}(t_1) & \cdots & \phi_{i,N}(t_1) \\ \phi_{i,1}(t_2) & \phi_{i,2}(t_2) & \cdots & \phi_{i,N}(t_2) \\ \cdots & \cdots & \cdots & \cdots \\ \phi_{i,1}(t_M) & \phi_{i,2}(t_M) & \cdots & \phi_{i,N}(t_M) \end{pmatrix} \tag{11}$$

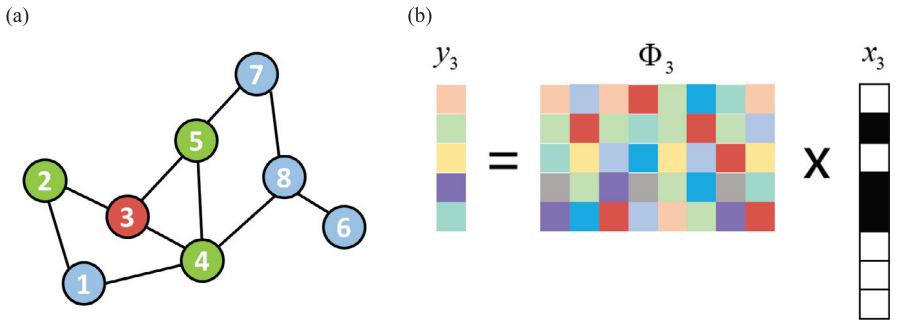

Fig. 1. Illustration of reconstructing the local topology of a focal node. (a) Example of an artificial game network with 8 nodes. (b) Relationship between the payoff vector and strategy matrix of node #3 (red) with $y_3 = \Phi_3 \cdot x_3$ from time series. Vector x_3 reflects the connection relationship between node #3 (red) and the other nodes in the network. Node #2, #4 and #5 (green) are direct neighbors. Accurate reconstruction result can be obtained when the second, fourth and fifth elements in vector x_3 which corresponds to interactions with #2, #4 and #5 are nonzero (black) while others are zero (white).

and the neighboring vector

$$\mathbf{x}_i = \begin{pmatrix} x_{i,1} & x_{i,2} & \cdots & x_{i,N} \end{pmatrix}^T \tag{12}$$

Therefore, with the collected $\mathbf{y}_i$ and $\mathbf{\Phi}_i$ from time series data, the goal of reconstructing the underlying topological network structure can be decomposed into several components, and solving each component can be translated as recovering a sparse signal, where the CS reconstruction framework discussed above can come in handy. In a similar fashion, the neighboring vectors for all nodes can be obtained separately, yielding a combined matrix as

$$\mathbf{A} = \begin{pmatrix} \mathbf{x}_1 & \mathbf{x}_2 & \cdots & \mathbf{x}_N \end{pmatrix} \tag{13}$$

where $\mathbf{A}$ is the so-called adjacency matrix. Thus the complete underlying topological network structure has been reconstructed successfully. An intuitive illustration of topology reconstruction process is shown in Fig. 1.

2.3. Sparse Bayesian learning-based network structure reconstruction

Based on above discussions, consider a general model [54] where the multiple observations are assumed to be contaminated with additive noise in the sampling process, which can be expressed based on the CS framework inspired by Ref. [15] as

$$\mathbf{Y} = \mathbf{\Phi}\mathbf{x} + \varepsilon \tag{14}$$

where $\mathbf{Y} = (\mathbf{y}_1, \ldots, \mathbf{y}_N)^T$ represents the sampling payoff vector. The strategy measurement matrix $\mathbf{\Phi}$ can be denoted by

$$\mathbf{\Phi} = \begin{pmatrix} \mathbf{\Phi}_1 & 0 & \cdots & 0 \\ 0 & \mathbf{\Phi}_2 & \cdots & 0 \\ \cdots & \cdots & \cdots & \cdots \\ 0 & 0 & \cdots & \mathbf{\Phi}_N \end{pmatrix} \tag{15}$$

$\mathbf{X} = vec(\mathbf{A}) = (\mathbf{x}_1, \ldots, \mathbf{x}_N)^T$ represents the vectorization of network adjacency matrix to be estimated, where vectors $\mathbf{x}_i$ is the ith column of adjacency matrix $\mathbf{A}$ according to Eq. (13). ε represents an additive noise perturbation to $\mathbf{Y}$. Specifically, each element of ε is independent in the sampling process and is conventionally assumed to be a zero-mean Gaussian noise with unknown variance σ^2, namely $\varepsilon_i \sim \mathcal{N}(\varepsilon_i|0, \sigma^2)$. Hence, we can obtain the associated Gaussian likelihood over $\mathbf{Y}$ as

$$\begin{aligned} p(\mathbf{Y}|\mathbf{X}, \sigma^2) &= \mathcal{N}(\mathbf{Y}|\mathbf{\Phi}\mathbf{x}, \sigma^2\mathbf{I}) \\ &= (2\pi\sigma^2)^{-MN/2} \exp\left\{-\frac{1}{2\sigma^2}\|\mathbf{Y} - \mathbf{\Phi}\mathbf{x}\|_2^2\right\} \end{aligned} \tag{16}$$

So far, the CS problem of inverting for $\mathbf{X}$ has been transformed into a Bayesian linear-regression analysis with a constraint of sparsity on $\mathbf{X}$ and the goal is to estimate $\mathbf{X}$ and the noise variance σ^2 based on the measurement $\mathbf{Y}$ [23]. Many related works have confirmed that, in a Bayesian formulation, the sparisity of variables is formalized by a sparseness-promoting prior [23,55–57] wherein the most widely used one is the Laplace prior [56]. However, since the Laplace prior is not conjugated to the Gaussian likelihood, it is difficult to carry the Bayesian analysis in closed form to accomplish an estimate of the full posterior on unknowns by using this prior directly [58,59]. Therefore, a framework of sparse Bayesian learning derived by the *relevance vector machine* (RVM) [19] has been employed in this scene, where a hierarchical prior

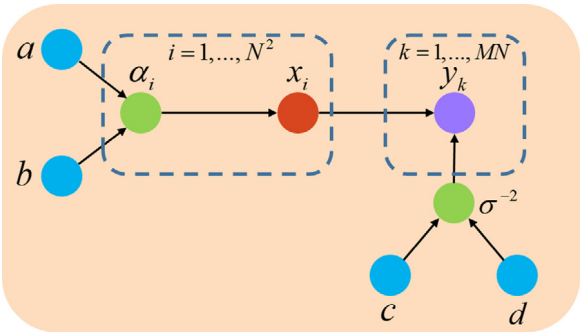

Fig. 2. Graphical structure of the hierarchical prior model. The payoff entries y_k, $k = 1, \ldots, MN$ of sampling payoff vector $\mathbf{Y}$ are observed variables and elements x_i, $i = 1, \ldots, N^2$ are unknown variables to be estimated. Besides, α_i, $i = 1, \ldots, N^2$ and σ^{-2} are hyperparameters and a, b, c, d are hyper-hyperparameters.

has been invoked on $\mathbf{X}$ for a convenient conjugated-analysis [19,23]. To be concrete, continued from the preceding, we firstly assign a Gaussian prior with zero-mean on each element of $\mathbf{X}$ as

$$p(\mathbf{X}|\alpha) = \prod_{i=1}^{N^2} \mathcal{N}(x_i|0, \alpha_i^{-1}) \tag{17}$$

where α_i represents the inverse-variance associated with each variable x_i independently. Further, in the second stage of the hierarchical model, a Gamma prior is considered over α as

$$p(\alpha) = \prod_{i=1}^{N^2} \text{Gamma}(\alpha_i|a, b) = \prod_{i=1}^{N^2} \Gamma(a)^{-1} b^a \alpha_i^{a-1} e^{-b\alpha_i} \tag{18}$$

and likewise over the noise variance σ^2 as

$$p(\beta) = \text{Gamma}(\beta|c, d) = \Gamma(c)^{-1} d^c \beta^{c-1} e^{-d\beta} \tag{19}$$

where $\beta \equiv \frac{1}{\sigma^2}$ and the Gamma function is $\Gamma(a) = \int_0^\infty t^{a-1} e^{-t} dt$. The graphical structure of the hierarchical prior model is reflected in Fig. 2.

With the prior defined in Eq. (17) and Gaussian likelihood in Eq. (16), the posterior distribution over $\mathbf{X}$ multiplied by two Gaussian can be obtained according to the probability theory

$$p(\mathbf{X}|\alpha, \sigma^2, \mathbf{Y}) = \frac{p(\mathbf{Y}|\mathbf{X}, \sigma^2) p(\mathbf{X}|\alpha)}{p(\mathbf{Y}|\alpha, \sigma^2)} \tag{20}$$

where the mean and covariance of the multivariate Gaussian posterior distribution $\mathcal{N}(\mathbf{X}|\mu, \mathbf{\Sigma})$ in Eq. (20) are expressed by Eqs. (21) and (22) respectively

$$\mu = \beta \mathbf{\Sigma} \mathbf{\Phi}^T \mathbf{Y} \tag{21}$$

$$\mathbf{\Sigma} = (\beta \mathbf{\Phi}^T \mathbf{\Phi} + \mathbf{\Lambda})^{-1} \tag{22}$$

with

$$\mathbf{\Lambda} = \text{diag}(\alpha_i), i = 1, \ldots, N^2 \tag{23}$$

Therefore, thanks to the hierarchical prior model constructed above, the problem of inferring posterior of target variables $\mathbf{X}$ has be formulated with unknown hyperparameters and multiple sampling data in closed form analytically. The question of interest raised here is that how to infer the unknown hyperparameters to achieve the posterior of $\mathbf{X}$. Here, a type-II maximum likelihood procedure in the context of *relevance vector machine* (RVM) [19] is employed to estimate the unknown parameters based on the above analysis. To be concrete, implement a marginalization procedure on the marginal likelihood over $\mathbf{X}$ for α and β, where the logarithm form can be expressed by

$$\begin{aligned} \ell(\alpha, \beta) &= \log p(\mathbf{Y}|\alpha, \beta) \\ &= \log \int p(\mathbf{Y}|\mathbf{x}, \beta) p(\mathbf{x}|\alpha) d\mathbf{x} \\ &= -\frac{1}{2}[K \log 2\pi + \log |\mathbf{C}| + \mathbf{Y}^T \mathbf{C}^{-1} \mathbf{Y}] \end{aligned} \tag{24}$$

with

$$\mathbf{C} = \beta^{-1}\mathbf{I} + \mathbf{\Phi}\mathbf{\Lambda}^{-1}\mathbf{\Phi}^{T} \tag{25}$$

where $\mathbf{I}$ is the identity matrix. Take the partial derivative of Eq. (24) over α and β respectively, equate to zero and then arrange the equation, obtaining the point estimates for each entry of α and β [23]. The iterative formulation can be obtained by Eqs. (26) and (27), respectively

$$\alpha_i^{new} = \frac{\gamma_i}{\mu_i^2} \tag{26}$$

$$\beta^{new} = \frac{N - \sum_i \gamma_i}{\|\mathbf{Y} - \mathbf{\Phi}\mathbf{x}\|_2^2} \tag{27}$$

with

$$\gamma_i \equiv 1 - \alpha_i \mathbf{\Sigma}_{ii} \tag{28}$$

where μ_i represents the ith posterior mean in Eq. (21) and $\mathbf{\Sigma}_{ii}$ represents the ith diagonal element of the posterior covariance in Eq. (22).

It should be pointed out that a mutual functional relationship between α, β in Eqs. (26) and (27) and μ, $\mathbf{\Sigma}$ in Eqs. (21) and (22) has emerged obviously, which implies an iterative estimation procedure can proceed until convergence criterions have been satisfied [19,23]. Hence the mean $\hat{\mu}$ of the output result is regarded as the point estimate and covariance $\hat{\mathbf{\Sigma}}$ as the inferring credibility of the reconstructed result. Thus, profiting from the hierarchical prior model which promotes the sparseness of $\mathbf{X}$ and the iterative estimation procedure in the parameter calculation process, the framework of sparse Bayesian learning has been implemented in the reconstruction process smoothly. The critical steps of sparse Bayesian learning-based network topology reconstruction algorithm are summarized in Algorithm 1.

Algorithm 1 Sparse Bayesian Learning-based Network Topology Reconstruction Algorithm

Require:
payoff sampling vector: $\mathbf{Y}$
strategy measurement matrix $\mathbf{\Phi}$
maximum number of iterations S_{max}
Ensure:
$\beta \equiv \sigma^{-2}$
$\gamma_i \equiv 1 - \alpha_i \mathbf{\Sigma}_{ii}$
Initialize: α, σ^2, μ, $\mathbf{\Sigma}$, $\mathbf{\Lambda}$, *iter*.
while if not converged **and** *iter* $\leq S_{max}$ **do**
  calculate: $\mu \leftarrow \beta \mathbf{\Sigma} \mathbf{\Phi}^T \mathbf{Y}$
  calculate: $\mathbf{\Sigma} \leftarrow (\beta \mathbf{\Phi}^T \mathbf{\Phi} + \mathbf{\Lambda})^{-1}$, $\mathbf{\Lambda} \leftarrow \mathrm{diag}(\alpha_i)$. $(i = 1, ..., N^2)$
  for $i = 1 \rightarrow N^2$ **do**
    calculate: $\alpha_i^{new} \leftarrow \frac{\gamma_i}{\mu_i^2}$
    calculate: $\beta^{new} \leftarrow \frac{N - \sum_i \gamma_i}{\|\mathbf{Y} - \mathbf{\Phi}\mathbf{x}\|_2^2}$
  end for
  iter $\leftarrow$ *iter* $+ 1$
  Check for convergence **and** *iter*
end while
return reconstructed mean $\hat{\mu}$, covariance $\hat{\mathbf{\Sigma}}$

3. Numerical results

In this section, numerical experiments are conducted to illustrate the performance of the proposed algorithm, also referred to as SBL. To be concrete, according to the principle of Monte Carlo simulation, we will run the evolutionary networked prisoner's dilemma game repeatedly based on an original network and then record the time series, including payoffs and strategies, during the evolution toward steady-state. After that, we will implement the proposed method based on the generated data to reconstruct the underlying topological network structure with the standard of adjacency matrix. The specific experiment processes are structured as follows. We first analyze the effectiveness of the proposed method with an intuitive visual example. Afterwards, we set different experimental conditions to verify the reconstruction performance from various aspects. Finally, we highlight the advantage and superiority of the proposed method compared with other reconstruction algorithms. We used MATLAB 2018a to run the simulations on a PC with an Intel Core i7-7700 3.60 GHz CPU and 8.0 GB RAM.

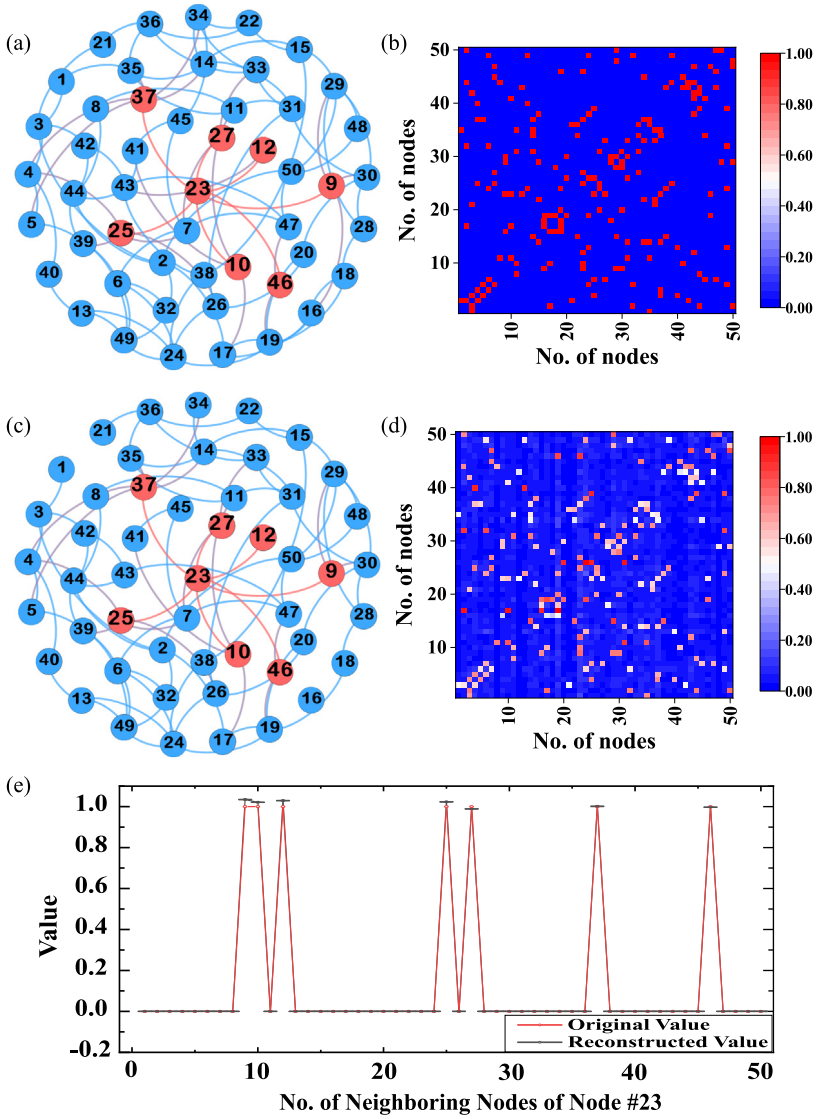

Fig. 3. Network structure reconstruction illustration. (a) The original visual structure scheme and (b) the corresponding heat map of adjacency matrix of the original network model. (c) The reconstructed visual structure scheme and (d) the corresponding heat map of adjacency matrix of the reconstructed network. Node #23 is the so-called hub node in the network. (e) Comparison of the reconstructed value and original value of link connections between node #23 and its neighboring nodes. The network model size is set to 50 and the average degree is $\langle k \rangle = 4$. It can be preliminarily seen that the proposed method performs well in network structure reconstruction.

A. Ability to reconstruct the underlying topological network structure

First, without loss of generality, we work with the Watts–Strogatz (WS) small-world network [60] in the first part of the experiment. Fig. 3(a) shows the visual structure scheme of the original network, and the heat map of adjacency matrix is presented in Fig. 3(b). Here, node #23 is the so-called hub node whose links are denser than those of other nodes, which is the most important supporting node in the network. Intuitively, nodes of #9, #10, #12, #25, #27, #37, #46 are included in the neighbor set of node #23, which is denoted by $\Gamma_{\#23}$. Afterwards, Monte Carlo simulations are performed on the network and networked evolutionary game data of each round, including payoffs and strategies, are recorded for reconstructing network structure via the proposed algorithm. The reconstructed network structure and the heat map of the corresponding adjacency matrix are shown in Fig. 3(c) and Fig. 3(d). Comparison of structure schemes and adjacency matrices between the original network and reconstructed network have demonstrated the effectiveness of the proposed method due to the fact that most of the link connections have been recovered perfectly for relatively accurate values and positions. Fig. 3(e) is a comparison of the reconstructed value and original value of link connections between node #23 and its neighboring nodes. The original value represents the value of link connections between node #23 and its neighboring

Table 1
Confusion matrix of the two-class classification problem.

		Actual label	
		Target class	Negative class
Predicted label	Target class	*TP*	*FP*
	Negative class	*FN*	*TN*

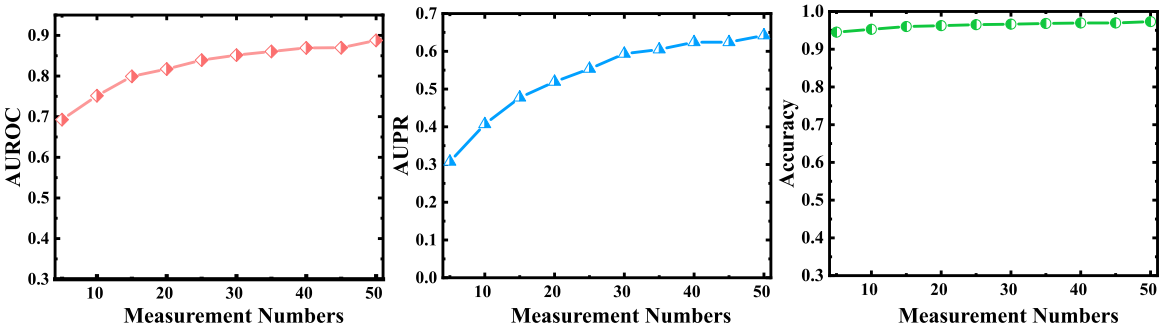

Fig. 4. AUROC, AUPR and Accuracy of the inferring network versus measurement numbers. The magnitudes Gaussian noise is 9% and the network size is $N = 50$. Each point is an average over 50 independent realizations. High indexes indicate a strong capability of the proposed method in reconstructing the underlying structure of network.

nodes in the original network, where the value is equal to 1 if there is a link between them, otherwise, the value is equal to 0. Meanwhile, the reconstructed value represents the value of link connections between node #23 and its neighboring nodes in the reconstructed network, wherein the point estimate is reflected by the mean of the reconstructed result and the inferring credibility by the covariance. Within the reasonable range of covariance fluctuation, we have strong confidence to believe that the reconstructed results are reliable near the mean value. Therefore, for the most important focal node #23 in the network, it is of great confidence that the neighboring nodes in $\Gamma_{\#23}$ have been found precisely. So far, it can be preliminarily seen that the proposed method performs well in the scene of reconstructing the underlying structure of network. For further verification of the proposed method, more investigations and explorations are needed, which will be presented in the following subsections.

B. Analysis of reconstruction performance for different data volumes

To systematically quantify the effectiveness of the proposed method in uncovering the underlying topological structure, we introduce the Accuracy, a global reconstruction index which measures the success rates in identifying both existent links and nonexistent links, to evaluate the reconstruction performance. Links are deemed to exist if the corresponding element in the reconstructed adjacency matrix is close to 1. In similar fashion, the element close to 0 means there exists no link. Note that without loss of generality, a threshold of 0.1 is assigned in the assessment process. A confusion matrix illustrated in Table 1 is used to classify the possible links into existent or nonexistent. Therefore, the index of Accuracy in network structure reconstruction can be defined as

$$Accuracy = \frac{TP + TN}{TP + FP + FN + TN} \tag{29}$$

where *TP* represents true positive, *TN* represents true negative, *FP* represents false positive and *FN* represents false negative. In addition, another two standard measures: AUROC, Area under the Receiver Operating Characteristic (ROC) curve [61], and AUPR, Area under the Precision–Recall (PR) curve [62] are employed as reconstruction performance indexes in the experiments as well.

The length of time series required in the process of network structure reconstruction is an important factor reflecting the effectiveness of the algorithm. Fig. 4 shows indexes of AUROC, AUPR and Accuracy as functions of measurement numbers based on the mentioned network model. As observed from Fig. 4, values of AUROC and AUPR will get higher as the amount of measurement number increases, and so is the Accuracy. It is worth mentioning that a perfect network structure reconstruction performance has been achieved with extremely few measurement numbers. For instance, with measurement numbers of 20, AUROC has reached 0.817 meanwhile AUPR has reached 0.519. What is more, the Accuracy of network structure reconstruction has been as high as 96.2%. The results shown in Fig. 4 has confirmed the effectiveness of the proposed method and demonstrated that although the available information is limited, a satisfactory reconstruction performance can also be obtained by the proposed algorithm. It is of great significance to achieve such a result because the requirement of an exceptionally small amount of data is particularly important for the situation where only rare information is available [6], which shows a strong capability of the proposed method in the scenario of network structure reconstruction.

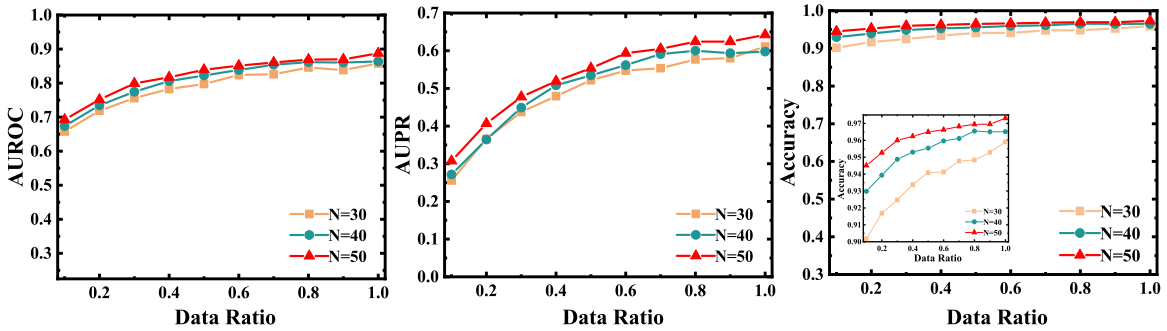

Fig. 5. AUROC, AUPR and Accuracy of three inferring networks with different network sizes versus the data ratio. N denotes the size of network which is set to 30, 40 and 50 for comparison. The magnitudes of Gaussian noise is 9% and the average degree is $\langle k\rangle = 4$. Each point is an average over 50 independent realizations. High indexes on larger networks indicate advantages of the proposed method in reconstructing the underlying structure of a large-scale network.

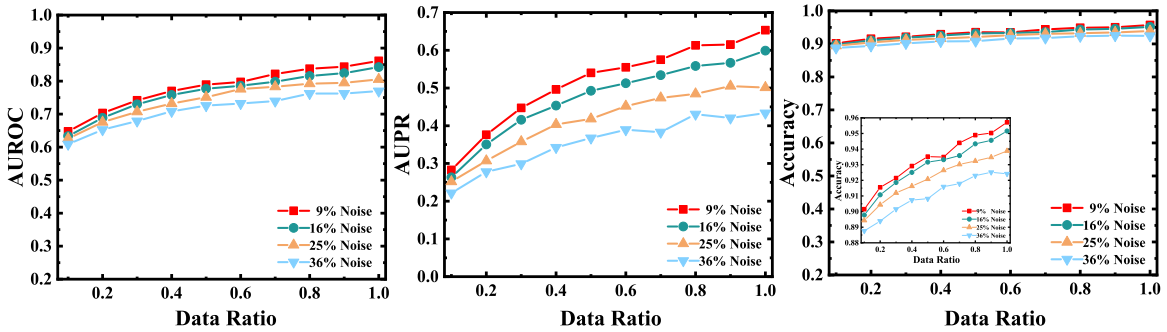

Fig. 6. AUROC, AUPR and Accuracy of the inferring network with different noisy magnitudes versus the data ratio. The noise magnitude is defined by the ratio of Gaussian noise amplitude σ_N to the payoff data and is set to 9%, 16%, 25% and 36% for comparison. The network size is $N = 30$ and the average degree is $\langle k\rangle = 4$. Each point is an average over 50 independent realizations. High indexes of network structure reconstruction against strong noise perturbations indicate the robustness of the proposed method.

C. Analysis of reconstruction performance for different network sizes

To further explore the effectiveness of the proposed method, different network sizes will be set up in this part. Fig. 5 depicts AUROC, AUPR and Accuracy of three inferring networks with different network sizes versus the data ratio, which is defined by M/N, where M denotes the number of accessible time instances in the time series and N denotes the network size. The size of network is set to 30, 40 and 50 for comparison. It can be confirmed that as the network size N increases, the reconstruction performance has been improved because all indicators increased with steady steps accordingly. In particular, the Accuracy, which represents a comprehensive index of the performance of network structure reconstruction, has been significantly improved in a larger network. Specifically, the Accuracy for a smaller network with size of $N = 30$ reaches 95% in case the data ratio is 0.9, whereas for a larger network with size of $N = 50$, only data ratio of 0.1 is needed to achieve the same Accuracy of 95%, which implies most of links have been uncovered successfully but with a quite smaller amount of information. Better performance on larger networks indicates that the proposed method has obvious advantages in solving reconstruction task of large-scale networks.

D. Analysis of robustness against Gaussian noise

In practice, noise is very common in various complex, networked, natural and social systems due to many uncertainties [63]. Besides, robustness is the basic requirement which allows complex networked system to maintain its functions despite internal and external perturbations in the field of science and engineering. Thus, exploring noise tolerance of the reconstruction process is an important aspect to evaluate the effectiveness of our algorithm. In this subsection, reconstruction of unknown networks with noise of different magnitudes on measurement data will be probed into based on the proposed algorithm. To be concrete, an additive Gaussian noise denoted by $[0, \sigma_N]$ is incorporated into the payoff data used for reconstruction realizations. Fig. 6 shows AUROC, AUPR and Accuracy of the inferring network versus the data ratio with different noise magnitudes. Note that the noise magnitude is defined by the ratio of Gaussian noise amplitude σ_N to the payoff data and is set to 9%, 16%, 25% and 36% for comparison. It can be observed that the performance of network structure reconstruction is less affected by strong Gaussian noise perturbations. Particularly, even when the noise magnitude is as high as 36%, which is a strong level of noise, AUROC still reaches 0.726, AUPR still reaches 0.367 and Accuracy still reaches 91.3% in case the data ratio is 0.5. Better reconstruction results can still be achieved from relatively small amount of time series against strong noise perturbations, providing strong evidence for the robustness

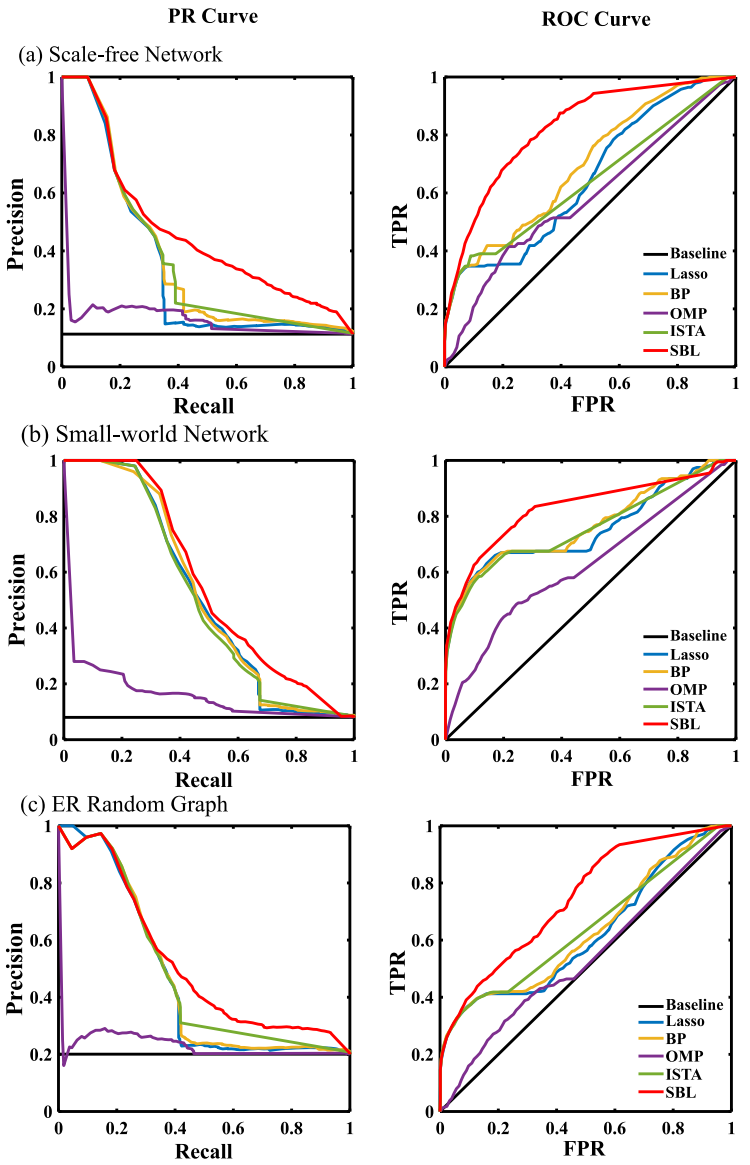

Fig. 7. PR graph and ROC graph for different network structure reconstruction methods on (a) scale-free network, (b) WS small-world network and (c) ER random graph. The magnitude of Gaussian noise is 9%, the network size is $N = 50$, the average degree is $\langle k \rangle = 4$ and the data ratio is 0.5. Each point is an average over 50 independent realizations. Higher indexes highlight the advantage and superiority of the proposed method.

of the proposed method. The immunity to Gaussian noise in our method has stressed the advantages in more practical scenarios.

E. Comparison of algorithms

To highlight the advantage and superiority of the proposed method, some other existing network structure reconstruction methods are employed for comparison by means of two standard measures, PR graph defined by true positive rate (TPR) versus false positive rate (FPR), and ROC graph defined by Precision versus Recall [61,62]. Fig. 7 presents the PR graph and ROC graph on scale-free network, small-world network and ER random graph for different reconstruction methods. It can be seen from the plots that the proposed method have presented the best reconstruction performance and outperformed the other algorithms. Furthermore, based on the PR graph and ROC graph in Fig. 7, the corresponding AUPR and AUROC of all reconstruction methods are summarized in Table 2, where the larger values of AUPR and AUROC of the proposed method have demonstrated better performance in network structure reconstruction. These results reassert the effectiveness of our method in solving network structure reconstruction tasks and can be attributed to the fact that compared to other reconstruction algorithms, the proposed method get free from the measurement correlation and model-based constraints, making reconstruction results more applicable and general.

Table 2
AUPR and AUROC measuring the performance of different methods for network structure reconstruction in small-world network, scale-free network and ER random graph.

	Small-world network		Scale-free network		ER random graph	
	AUPR	AUROC	AUPR	AUROC	AUPR	AUROC
Lasso	0.5121	0.7557	0.3475	0.6506	0.4574	0.6204
BP	0.5186	0.7692	0.3705	0.6961	0.4607	0.6308
OMP	0.1641	0.6242	0.1681	0.5837	0.2334	0.5350
ISTA	0.5067	0.7604	0.3745	0.6397	0.4774	0.6406
SBL	**0.5653**	**0.8309**	**0.4621**	**0.8255**	**0.5174**	**0.7451**

4. Conclusion and discussion

In conclusion, we proposed a new framework of sparse Bayesian learning for network structure reconstruction based on evolutionary game data in this paper. As one of the central issues and fundamental inverse problem in complex networked system, data-based network structure reconstruction plays an utmost significant role in interdisciplinary fields and attracts continuous interest. In the meanwhile, recent years have witnessed dramatic advances of network structure reconstruction in the framework of compressed sensing. However, some neglected disadvantages still exist and inevitably drag down the reconstruction performance somehow. Then, we developed a new framework of sparse Bayesian learning for network structure reconstruction, which is originated from *relevance vector machine* (RVM) in the machine learning literature. Specifically, we formulate the problem of reconstructing the underlying topological structure of network as a Bayesian compressed sensing problem. Later, a hierarchical prior model is invoked for conjugated Bayesian inference to obtain the posterior distribution of the reconstructed results, including the reconstructed mean and covariance. Finally, the unknown parameters are updated by an iterative estimation procedure.

It is a novel work to learn the underlying topological structure from limited measurement data. Results from numerical experiments have demonstrated applicability and efficiency of the proposed method from aspects of data requirement, performance under different network scales and robustness against strong noise. Furthermore, compared with some state-of-the-art network structure reconstruction algorithms, we highlight the advantage and present superiority of the proposed method with better reconstruction performance. Potential applications to be extended in the network engineering include: (a) firstly, we can make the best of less measurement data to reconstruct the underlying topological structure in the network engineering, especially in the research of protein networks, neural networks and other rigorous data measurement environments. (b) Secondly, we transform it into a root-finding problem, which can get free from the model-based constraints in the reconstruction behaviors and avoids deterioration in high noise level, obtaining more applicable and general reconstruction results. (c) Thirdly, in the framework of sparse Bayesian learning, the existence of credibility provided in each reconstruction process can take one-shot action as far as possible, eliminating the requirement of multiple measurements and computational costs. Our main work provides evidence for the research of Bayesian and statistical algorithms in solving the problem of practical topology reconstruction. Further design of hierarchical prior for specific network structure may supply strong support for effectively improving the accuracy of network structure reconstruction in the future. In a nutshell, this paper opens a new road to solve the important yet challenging problem of network structure reconstruction from the perspective of Bayesian and statistics.

Declaration of competing interest

The authors declare that they have no known competing financial interests or personal relationships that could have appeared to influence the work reported in this paper.

Acknowledgments

This work was supported in part by the National Natural Science Foundation of China (Grant Nos. 61703439, 61803232, 61751312, 61374156), in part by the Foundation for Innovative Research Groups of the National Natural Science Foundation of China (Grant No. 61621062), in part by the Innovation-Driven Plan in Central South University, China (2019CX020), and in part by the 111 Project, China (B17048).

References

[1] A.-L. Barabási, Taming complexity, Nat. Phys. 1 (2) (2005) 68.
[2] S. Boccaletti, V. Latora, Y. Moreno, M. Chavez, D.-U. Hwang, Complex networks: Structure and dynamics, Phys. Rep. 424 (4–5) (2006) 175–308.
[3] R. Cohen, S. Havlin, Complex Networks: Structure, Robustness and Function, Cambridge university press, 2010.
[4] T.S. Gardner, D. Di Bernardo, D. Lorenz, J.J. Collins, Inferring genetic networks and identifying compound mode of action via expression profiling, Science 301 (5629) (2003) 102–105.
[5] Z. Shen, W.-X. Wang, Y. Fan, Z. Di, Y.-C. Lai, Reconstructing propagation networks with natural diversity and identifying hidden sources, Nature Commun. 5 (2014) 4323.

[6] W.-X. Wang, Y.-C. Lai, C. Grebogi, J. Ye, Network reconstruction based on evolutionary-game data via compressive sensing, Phys. Rev. X 1 (2) (2011) 021021.
[7] X. Han, Z. Shen, W.-X. Wang, Z. Di, Robust reconstruction of complex networks from sparse data, Phys. Rev. Lett. 114 (2) (2015) 028701.
[8] A.-L. Barabási, The network takeover, Nat. Phys. 8 (1) (2011) 14.
[9] G. Li, X. Wu, J. Liu, J.-a. Lu, C. Guo, Recovering network topologies via taylor expansion and compressive sensing, Chaos 25 (4) (2015) 043102.
[10] S. Hempel, A. Koseska, J. Kurths, Z. Nikoloski, Inner composition alignment for inferring directed networks from short time series, Phys. Rev. Lett. 107 (5) (2011) 054101.
[11] X. Han, Z. Shen, W.-X. Wang, Y.-C. Lai, C. Grebogi, Reconstructing direct and indirect interactions in networked public goods game, Sci. Rep. 6 (2016) 30241.
[12] J. Ren, W.-X. Wang, B. Li, Y.-C. Lai, Noise bridges dynamical correlation and topology in coupled oscillator networks, Phys. Rev. Lett. 104 (5) (2010) 058701.
[13] W.-X. Wang, Q. Chen, L. Huang, Y.-C. Lai, M.A.F. Harrison, Scaling of noisy fluctuations in complex networks and applications to network prediction, Phys. Rev. E 80 (1) (2009) 016116.
[14] Y. Yuan, G.-B. Stan, S. Warnick, J. Gonçalves, Robust dynamical network reconstruction, in: 49th IEEE Conference on Decision and Control (CDC), IEEE, 2010, pp. 810–815.
[15] K. Huang, Z. Wang, M. Jusup, Incorporating latent constraints to enhance inference of network structure, IEEE Trans. Netw. Sci. Eng. (2018).
[16] R.-Q. Su, W.-X. Wang, Y.-C. Lai, Detecting hidden nodes in complex networks from time series, Phys. Rev. E 85 (6) (2012) 065201.
[17] Y.C. Eldar, M. Mishali, Robust recovery of signals from a structured union of subspaces, IEEE Trans. Inform. Theory 55 (11) (2009) 5302–5316.
[18] Y.C. Eldar, P. Kuppinger, H. Bolcskei, Block-sparse signals: Uncertainty relations and efficient recovery, IEEE Trans. Signal Process. 58 (6) (2010) 3042–3054.
[19] M.E. Tipping, Sparse bayesian learning and the relevance vector machine, J. Mach. Learn. Res. 1 (Jun) (2001) 211–244.
[20] D.P. Wipf, B.D. Rao, An empirical bayesian strategy for solving the simultaneous sparse approximation problem, IEEE Trans. Signal Process. 55 (7) (2007) 3704–3716.
[21] D.P. Wipf, B.D. Rao, S. Nagarajan, Latent variable bayesian models for promoting sparsity, IEEE Trans. Inform. Theory 57 (9) (2011) 6236–6255.
[22] G. Tzagkarakis, D. Milioris, P. Tsakalides, Multiple-measurement bayesian compressed sensing using gsm priors for doa estimation, in: 2010 IEEE International Conference on Acoustics, Speech and Signal Processing, IEEE, 2010, pp. 2610–2613.
[23] S. Ji, Y. Xue, L. Carin, et al., Bayesian compressive sensing, IEEE Trans. Signal Process. 56 (6) (2008) 2346.
[24] D.P. Wipf, B.D. Rao, Sparse bayesian learning for basis selection, IEEE Trans. Signal Process. 52 (8) (2004) 2153–2164.
[25] Z. Zhang, B.D. Rao, Sparse signal recovery with temporally correlated source vectors using sparse bayesian learning, IEEE J. Sel. Top. Sign. Proces. 5 (5) (2011) 912–926.
[26] J. Fang, Y. Shen, H. Li, P. Wang, Pattern-coupled sparse bayesian learning for recovery of block-sparse signals, IEEE Trans. Signal Process. 63 (2) (2014) 360–372.
[27] M.O. Ahmed, L. Lampe, Power line communications for low-voltage power grid tomography, IEEE Trans. Commun. 61 (12) (2013) 5163–5175.
[28] X. Ma, F. Yang, W. Ding, J. Song, Topology reconstruction for power line network based on bayesian compressed sensing, in: 2015 IEEE International Symposium on Power Line Communications and Its Applications (ISPLC), IEEE, 2015, pp. 119–124.
[29] S.S. Chen, D.L. Donoho, M.A. Saunders, Atomic decomposition by basis pursuit, SIAM Rev. 43 (1) (2001) 129–159.
[30] J.A. Tropp, A.C. Gilbert, Signal recovery from random measurements via orthogonal matching pursuit, IEEE Trans. Inform. Theory 53 (12) (2007) 4655–4666.
[31] A. Beck, M. Teboulle, Gradient-based algorithms with applications to signal recovery, in: Convex Optimization in Signal Processing and Communications, 2009, pp. 42–88.
[32] J. Ren, W.-X. Wang, F. Qi, Randomness enhances cooperation: A resonance-type phenomenon in evolutionary games, Phys. Rev. E 75 (4) (2007) 045101.
[33] Z. Wang, C.-Y. Xia, S. Meloni, C.-S. Zhou, Y. Moreno, Impact of social punishment on cooperative behavior in complex networks, Sci. Rep. 3 (2013) 3055.
[34] F.C. Santos, J.M. Pacheco, T. Lenaerts, Evolutionary dynamics of social dilemmas in structured heterogeneous populations, Proc. Natl. Acad. Sci. 103 (9) (2006) 3490–3494.
[35] Z. Wang, C.T. Bauch, S. Bhattacharyya, A. d'Onofrio, P. Manfredi, M. Perc, N. Perra, M. Salathe, D. Zhao, Statistical physics of vaccination, Phys. Rep. 664 (2016) 1–113.
[36] M. Perc, J.J. Jordan, D.G. Rand, Z. Wang, S. Boccaletti, A. Szolnoki, Statistical physics of human cooperation, Phys. Rep. 687 (2017) 1–51.
[37] M.R. D'Orsogna, M. Perc, Statistical physics of crime: A review, Phys. Life Rev. 12 (2015) 1–21.
[38] D. Helbing, D. Brockmann, T. Chadefaux, K. Donnay, U. Blanke, O. Woolley-Meza, M. Moussaid, A. Johansson, J. Krause, S. Schutte, et al., Saving human lives: What complexity science and information systems can contribute, J. Stat. Phys. 158 (3) (2015) 735–781.
[39] J. Hofbauer, K. Sigmund, Evolutionary game dynamics, Bull. Amer. Math. Soc. 40 (4) (2003) 479–519.
[40] C.P. Roca, J.A. Cuesta, A. Sánchez, Evolutionary game theory: Temporal and spatial effects beyond replicator dynamics, Phys. Life Rev. 6 (4) (2009) 208–249.
[41] M. Perc, A. Szolnoki, Coevolutionary games—a mini review, BioSystems 99 (2) (2010) 109–125.
[42] Z. Wang, L. Wang, A. Szolnoki, M. Perc, Evolutionary games on multilayer networks: a colloquium, Eur. Phys. J. B 88 (5) (2015) 124.
[43] F.C. Santos, J.M. Pacheco, A new route to the evolution of cooperation, J. Evol. Biol. 19 (3) (2006) 726–733.
[44] M. Perc, Double resonance in cooperation induced by noise and network variation for an evolutionary prisoner's dilemma, New J. Phys. 8 (9) (2006) 183.
[45] K. Wu, J. Liu, Evolutionary game network reconstruction by memetic algorithm with l 1/2 regularization, in: Asia-Pacific Conference on Simulated Evolution and Learning, Springer, 2017, pp. 15–26.
[46] L. Ma, X. Han, Z. Shen, W.-X. Wang, Z. Di, Efficient reconstruction of heterogeneous networks from time series via compressed sensing, PLoS One 10 (11) (2015) e0142837.
[47] E.J. Candes, J. Romberg, T. Tao, Robust uncertainty principles: Exact signal reconstruction from highly incomplete frequency information, IEEE Trans. Inform. Theory 52 (2) (2006) 489–509.
[48] D.L. Donoho, et al., Compressed sensing, IEEE Trans. Inform. Theory 52 (4) (2006) 1289–1306.
[49] L. Gan, Block compressed sensing of natural images, in: 2007 15th International Conference on Digital Signal Processing, IEEE, 2007, pp. 403–406.
[50] M.F. Duarte, Y.C. Eldar, Structured compressed sensing: From theory to applications, IEEE Trans. Signal Process. 59 (9) (2011) 4053–4085.
[51] E.J. Candes, The restricted isometry property and its implications for compressed sensing, C. R. Math. 346 (9–10) (2008) 589–592.
[52] E.J. Candès, M.B. Wakin, An introduction to compressive sampling [a sensing/sampling paradigm that goes against the common knowledge in data acquisition], IEEE Signal Process. Mag. 25 (2) (2008) 21–30.
[53] T. Hastie, R. Tibshirani, J. Friedman, J. Franklin, The elements of statistical learning: data mining, inference and prediction, Math. Intell. 27 (2) (2005) 83–85.

[54] S.F. Cotter, B.D. Rao, K. Engan, K. Kreutz-Delgado, Sparse solutions to linear inverse problems with multiple measurement vectors, IEEE Trans. Signal Process. 53 (7) (2005) 2477–2488.
[55] L. He, L. Carin, Exploiting structure in wavelet-based bayesian compressive sensing, IEEE Trans. Signal Process. 57 (9) (2009) 3488–3497.
[56] S.D. Babacan, R. Molina, A.K. Katsaggelos, Bayesian compressive sensing using laplace priors, IEEE Trans. Image Process. 19 (1) (2009) 53–63.
[57] L. Yu, H. Sun, J.-P. Barbot, G. Zheng, Bayesian compressive sensing for cluster structured sparse signals, Signal Process. 92 (1) (2012) 259–269.
[58] J.M. Bernardo, A.F. Smith, Bayesian Theory, Vol. 405, John Wiley & Sons, 2009.
[59] A. Gelman, J.B. Carlin, H.S. Stern, D.B. Dunson, A. Vehtari, D.B. Rubin, Bayesian Data Analysis, Chapman and Hall/CRC, 2013.
[60] D.J. Watts, S.H. Strogatz, Collective dynamics of 'small-world'networks, Nature 393 (6684) (1998) 440.
[61] J. Huang, C.X. Ling, Using auc and accuracy in evaluating learning algorithms, IEEE Trans. Knowl. Data Eng. 17 (3) (2005) 299–310.
[62] J. Davis, M. Goadrich, The relationship between precision-recall and roc curves, in: Proceedings of the 23rd International Conference on Machine Learning, ACM, 2006, pp. 233–240.
[63] P.S. Swain, A. Longtin, Noise in genetic and neural networks, Chaos 16 (2) (2006) 026101.